JACS
JOURNAL OF THE AMERICAN CHEMICAL SOCIETY
Article
pubs.acs.org/JACS

Performance of Fe−N/C Oxygen Reduction Electrocatalysts toward NO_2^-, NO, and NH_2OH Electroreduction: From Fundamental Insights into the Active Center to a New Method for Environmental Nitrite Destruction

Daniel Malko,[†] Anthony Kucernak,*[,†] and Thiago Lopes[‡]

[†]Department of Chemistry, Imperial College London, South Kensington Campus, London SW7 2AZ, United Kingdom
[‡]Fuel Cells and Hydrogen Center, Nuclear and Energy Research Institute, IPEN-CNEN/SP, Sao Paulo-SP 05508-000, Brazil

Supporting Information

ABSTRACT: Although major progress has recently been achieved through ex situ methods, there is still a lack of understanding of the behavior of the active center in non-precious metal Fe−N/C catalysts under operating conditions. Utilizing nitrite, nitric oxide, and hydroxylamine as molecular probes, we show that the active site for the oxygen reduction reaction (ORR) is different under acidic and alkaline conditions. An in-depth investigation of the ORR in acid reveals a behavior which is similar to that of iron macrocyclic complexes and suggests a contribution of the metal center in the catalytic cycle. We also show that this catalyst is highly active toward nitrite and nitric oxide electroreduction under various pH values with ammonia as a significant byproduct. This study offers fundamental insight into the chemical behavior of the active site and demonstrates a possible use of these materials for nitrite and nitric oxide sensing applications or environmental nitrite destruction.

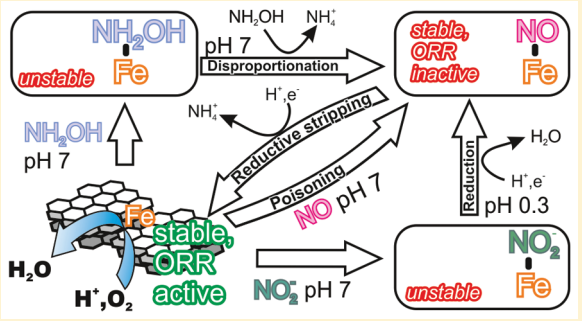

1. INTRODUCTION

Polymer electrolyte fuel cells and other renewable energy technologies rely heavily on electrocatalysts for the oxygen reduction reaction (ORR).[1] One major obstacle in the commercialization is the large amount of expensive and scarce Pt at the cathode to catalyze the ORR.[1] Promising materials to replace precious metals are pyrolized iron and nitrogen doped carbon catalysts.[2−6] These materials emerged after the discovery by Jasinski that cobalt-phthalocyanine and also other transition metal macrocycles were capable of catalyzing the ORR.[7−11] Later, it was found that a heat treatment of these materials increases their stability and activity.[9,12,13] Numerous routes to these materials have subsequently been developed, and high activities in fuel cells have been demonstrated.[3,14] However, the activity of these materials is still too low, and further developments have been hindered by limited information on the active site and its chemical behavior.[14−16] It was not clear whether the macrocyclic moiety survives heat treatment or a similar structure, embedded into the carbon lattice as atomic metal, serves as the active site.[3,12] Recent studies suggest that atomic iron centers, which are coordinated with nitrogen and embedded into the carbon lattice, might serve as one major type of active site, as they were found to be present in most of the materials with the highest activities under acidic conditions.[17−23] This implies that these sites should chemically behave similarly to iron heme type systems and interact with molecules such as CO, NO, and H_2S.[24] Other possible active sites are carbon encapsulated iron or iron carbide particles or metal free nitrogen moieties in the carbon lattice which might not necessarily interact with these molecules.[25] Although significant progress has recently been made in establishing the active center(s), most studies only provide indirect evidence for the active site as the material is characterized ex situ with sophisticated procedures and experiments that are open to interpretation, such as X-ray absorption and Mössbauer spectroscopy,[18,20,21,26] and hence, establishing correlations is challenging. Electrochemically investigating the active site in situ is difficult and requires a probe that interacts strongly. There are some studies that investigate the effect of certain molecules on the activity of Fe−N/C catalysts (hence forth we use the term N/C to denote the iron-free nitrogen/carbon catalyst and Fe−N/C to denote the same catalyst with iron). Gupta et al. noted early on that cyanide in alkaline solution decreases the activity of iron macrocyclic compounds.[27] Thorum et al. investigated the effect of various small molecules on a pyrolyzed iron phthalocyanine catalyst under different conditions and also found that it is strongly inhibited upon cyanide treatment in alkaline solution.[28,29] Singh et al. studied the effect of H_2S on a pyrolyzed Fe−N/C catalyst and noted that ex situ treatment decreases the electrochemical activity.[30] They inferred an iron

Received: September 19, 2016
Published: November 13, 2016

DOI: 10.1021/jacs.6b09622
J. Am. Chem. Soc. 2016, 138, 16056−16068

Scheme 1. Typical Compounds of the Different Nitrogen Oxidation States Present in an Acidic Aqueous Solution in Descending Order of Oxidation State[a]

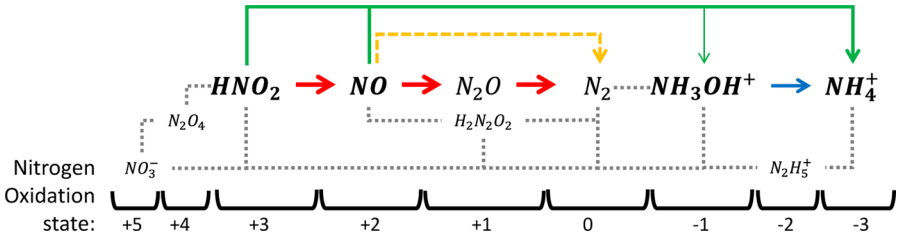

[a]The major pathways for nitrite and nitric oxide electroreduction are highlighted. Green and blue pathway: possible products and intermediates upon subsequent cleavage of N−O bonds without N−N bond formation. Red and yellow pathway: likely products and intermediates upon N−O cleavage with N−N bond formation. Grey dot pathway: kinetically hindered route.

centered structure as active site. However, there are also studies that suggest that iron might not necessarily be the active site.[31,32] The most prominent study that raised doubts on the active site was from the Dodelet group which did not find an electrochemical interaction of the catalyst with carbon monoxide an otherwise strong poison for iron.[33] We recently also reported on the peculiar poison tolerance of this type of catalyst to hydrogen sulfide, aromatic molecules (benzene, toluene), anions (chloride, phosphate), and methanol.[34] Although this insensitivity to poisons seems contradictory, it does not necessarily exclude a metallic active site. From metal complexes it is known that the structural and chemical environment significantly influences the affinity of the active site to certain substrates.[24] Another recent study investigates a broad spectrum of various small molecules such as anions, thiocyanide, CO, and NO_x.[35] It found a slight activity decrease with anions, a large effect of thiocyanate, and no interaction with CO and NO_x. An iron(III) center was proposed as active site as CO would only interact with iron(II). However, NO should interact with an iron(III) center.[36] Although these studies provided some information, no detailed study of the chemical and electrochemical behavior was presented. Ideally, a molecular probe that interacts with the active site forms stable adducts which are electrochemically accessible and behave differently depending on the external conditions. Such information would allow correlation of ex situ and in situ measurements and elucidate hitherto inaccessible trends, such as activities and densities of specific sites. This could lead to the structured synthesis of the site with the highest activity and the ability to overcome the currently insufficient performance. Molecules from the aqueous nitrogen cycle, such as nitric oxide or nitrite, are an attractive option. This is due to the fact that the nitrogen molecule exhibits a rich electrochemical behavior and can exist in 9 oxidation states.[37,38] As nitric oxide and nitrite have a tremendous importance for biological systems and environmental chemistry, their interaction with iron macrocycles has been extensively investigated.[24,39−45] The electrochemistry of nitrite and nitric oxide reduction is also well-documented for precious metal based catalysts.[38,44−50] The reduction of nitrite might be of an environmental benefit through the destruction of this pollutant; sensing applications are also of interest for biological systems.[38,51−53]

Scheme 1 shows the different oxidation states of nitrogen in aqueous solutions.[37] The compounds of interest for this study are highlighted in bold. It can be seen that there are different pathways for the electroreduction of nitrite and nitric oxide. The green and blue pathways involve N−O bond cleavage without N−N bond formation, while the yellow and red pathways include N−N bond formation.[38] In this study, we present a series of experiments that investigate the interaction of an Fe−N/C catalyst and an N/C catalyst with nitrite, hydroxylamine, and nitric oxide under various reaction conditions. We find that the chemical and electrochemical behavior observed can be explained using the chemistry of iron macrocycles. We also find that the Fe−N/C catalyst is highly active toward the electroreduction of nitrite and nitric oxide. The difference in overpotential for the Fe−N/C catalyst compared to the N/C catalyst is similar to the difference when performing the oxygen reduction reaction. Ammonia is a major byproduct and hydroxylamine only a minor byproduct. Besides introducing a new powerful substrate to study Fe−N/C catalysts, we demonstrate a highly active catalyst for the useful nitrite and nitric oxide reduction reaction, able to break both N−O bonds in the nitrite, which could be exploited in biological and environmental chemistry.[39,53]

2. MATERIALS AND METHODS

2.1. Synthesis of the Catalysts. The catalyst Fe−N/C was synthesized by dissolving 1.0 g (6.4 mmol) of 1,5-diaminonaphthalene (97%, Alfa Aesar), 1.0 g (4.4 mmol) of $(NH_4)_2S_2O_8$ (98%, Sigma-Aldrich), and 35.6 mg of $FeCl_2{\cdot}4H_2O$ (99%, Sigma-Aldrich) in 250 mL of ethanol (absolute, VWR). The solution was stirred for 24 h at room temperature. The solvent was then removed with a rotary evaporator. When dry, the resulting residue was transferred to an alumina boat (11 cm long by 2 cm wide by 1 cm deep, approximately 10 mL of volume capacity) and heat treated at 950 °C for 2 h, after reaching the end temperature, in a tube (quartz) furnace (Carbolite) at a heating rate of 20 °C/min. This heat treatment was performed in an inert atmosphere, under a continuous flow of nitrogen (50 ccm). After being cooled under nitrogen, the resulting material was removed from the quartz boat and refluxed in 0.5 M H_2SO_4 for 8 h, in order to remove any soluble metal phases. The material was then filtered and dried. The dried powder was then subjected to a second heat treatment at 900 °C for 2 h after reaching the target temperature at a heating rate of 20 °C/min under nitrogen and allowed to cool as above. The resulting powder was then ready to use. The catalyst N/C was synthesized in the same way without the addition of the metal salt.

2.2. Electrochemical Measurements. Measurements were conducted with a rotating ring disk electrode (Pine Instruments, model AFE6R1 AU, with a mirror polished glassy carbon disk and rotator model AFMSRCE); the catalyst was deposited on the glassy carbon disk as per a literature procedure.[54,55] The ink utilized consisted of 1 wt % catalyst in a 1:1 volume ratio mixture of IPA (VWR):H_2O (Milli-Q 18.2 MΩ cm) with a Nafion (5 wt%, Sigma Aldrich) to catalyst weight ratio of 1:1. This composition was found to give a uniform catalyst layer. A custom-made three compartment electrochemical glass cell was used. The reference electrode was ionically connected to the main compartment of the electrochemical glass cell via a Luggin−Haber capillary. For measurements in 0.5 M

DOI: 10.1021/jacs.6b09622
J. Am. Chem. Soc. 2016, 138, 16056−16068

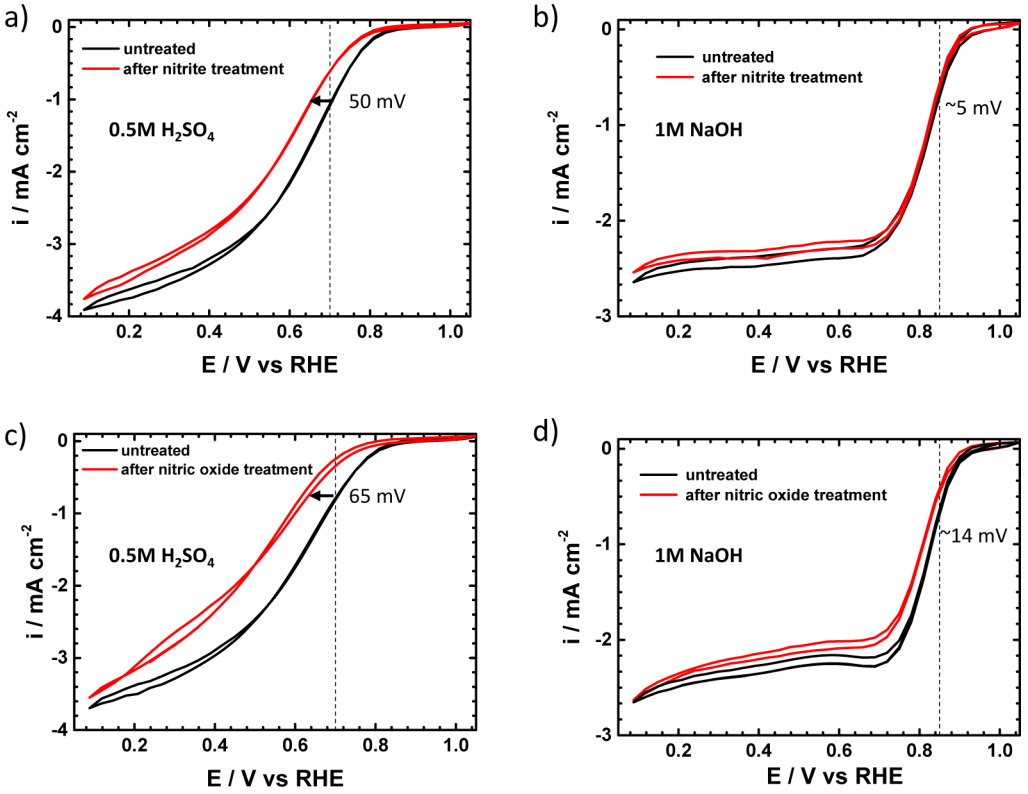

Figure 1. Rotating disk electrode (RDE) measurements of the ORR activity in acid (a, c) or base (b, d) of a Fe−N/C catalyst before (untreated) and after subjecting it to poisoning by a 0.125 M $NaNO_3$ solution at pH 7 (a, b), or nitric-oxide-saturated 0.5 M PO_4 at pH 7 (c, d). Conditions include RDE at 1600 rpm, catalyst loading at 270 μg cm^{-2}, scan rate at 5 mV/s, and O_2-saturated electrolytes. Electrodes were washed with DI water before immersion in electrolytes, 0.5 mol dm^{-3} H_2SO_4 or 1.0 mol dm^{-3} NaOH.

H_2SO_4, a RHE (GaskatelHydroFlex) was used. For measurements in the higher pH electrolytes, a saturated calomel electrode (SCE, VWR) was used, and the potentials with respect to the RHE scale were determined by measuring the change from hydrogen evolution to hydrogen oxidation in the respective H_2-saturated electrolyte on a platinized platinum wire. A glassy carbon rod was used as counter electrode and ionically connected to the main compartment of the glass cell through a porous frit. Glassy carbon was used instead of Pt in order to avoid contamination with catalytically active precious metals. A potentiostat (Autolab, PGSTAT20) was used for potential or current control during the electrochemical measurements. Ultrapure gases, nitrogen, oxygen, and hydrogen (BIP plus-X47S, Air products), were used. When nitric oxide (from BOC > 99%) was used, it was passed through 2 washing bottles filled with 3 M KOH (AnalaR Normapur, VWR). This was necessary in order to remove trace amounts of NO_2.[44] Before passing NO into the electrochemical cell, the electrolyte was degassed with nitrogen and blanketed afterward in order to avoid the reaction of NO with O_2.[56] Electrolytes were prepared in ultrapure water (Milli-Q 18.2 MΩ cm). Where deionized (DI) water is mentioned, ultrapure water (Milli-Q 18.2 MΩ cm) was used. These electrolytes were prepared as follows: 0.5 M H_2SO_4 from 95% sulfuric acid (Aristar, VWR), 0.5 M acetate buffer pH 5.2 from sodium acetate (99%, Sigma-Aldrich) and glacial acetic acid (AnalaR Normapur, VWR), 0.5 M phosphate buffer pH 7 from NaH_2PO_4 (AnalaR Normapur, VWR) and Na_2HPO_4 (AnalaR Normapur, VWR), 0.5 borate buffer pH 9 from boric acid (ACS reagent, 99.5%, Sigma-Aldrich) and NaOH (AnalaR Normapur, VWR), and 1 M NaOH from NaOH pellets (AnalaR Normapur, VWR). The pH was adjusted with 0.5 M NaOH and confirmed with a ROSS Ultra Glass pH Electrode (Orion 8102BNUWP). The nitrite solution was prepared from $NaNO_2$ (ACS reagent, 99%, Sigma-Aldrich), and the hydroxylamine solution was prepared from $NH_2OH{\cdot}HCl$ (ReagentPlus, 99%, Sigma-Aldrich) in pH 7 phosphate buffer. For the long-term electrolysis experiment, pH 5.2 0.05 M acetate buffer was prepared from potassium acetate (99%, Sigma-Aldrich) and glacial acetic acid (AnalaR Normapur, VWR), and the nitrite source was 0.01 M KNO_2 (VWR, 99%). The lower concentration and the use of potassium instead of sodium were necessary, as the low expected signal of ammonium would otherwise have been swamped by the large signal of sodium with a similar elution time (see Supporting Information). Exact steps for the series of treatments used in the different pathways can be found in the Supporting Information.

2.3. Poisoning Protocol. Detailed procedures are in SI sections S3, S6, S7, and S9. Briefly, the rotating disk electrode disk with deposited catalyst was washed in DI water and then immersed into a pH 7 solution of the respective poison (125 mM $NaNO_2$, NO-saturated 0.5 M phosphate buffer, 125 mM hydroxylamine solution) at open circuit potential (OCP) for 5 min under a rotation of 300 rpm, and then washed for 5 min under a rotation of 300 rpm.

3. RESULTS AND DISCUSSION

3.1. Interaction of the Fe−N/C Catalyst with Nitrogen Containing Poisons. The Fe−N/C catalyst and the N/C catalyst were prepared with an approach similar to that of a literature procedure.[34] 1,5-Diaminonaphtalene was oxidatively polymerized either in the presence of 1 wt % iron (Fe−N/C) or without the addition of a metal salt (N/C). The resulting nanoparticles were then heat treated under an inert atmosphere at 950 °C, acid leached, and then heat treated for a second time at 900 °C. The absence of a significant amount of particulate nanophases in the Fe−N/C catalyst was confirmed by high resolution TEM and STEM images (see Supporting Information section S1), and absence of such signals in the XRD. This means that the active sites present in this material are likely atomic iron sites coordinated with nitrogen,[18,20,23] as opposed to encapsulated metallic or carbide phases which

DOI: 10.1021/jacs.6b09622
J. Am. Chem. Soc. 2016, 138, 16056−16068

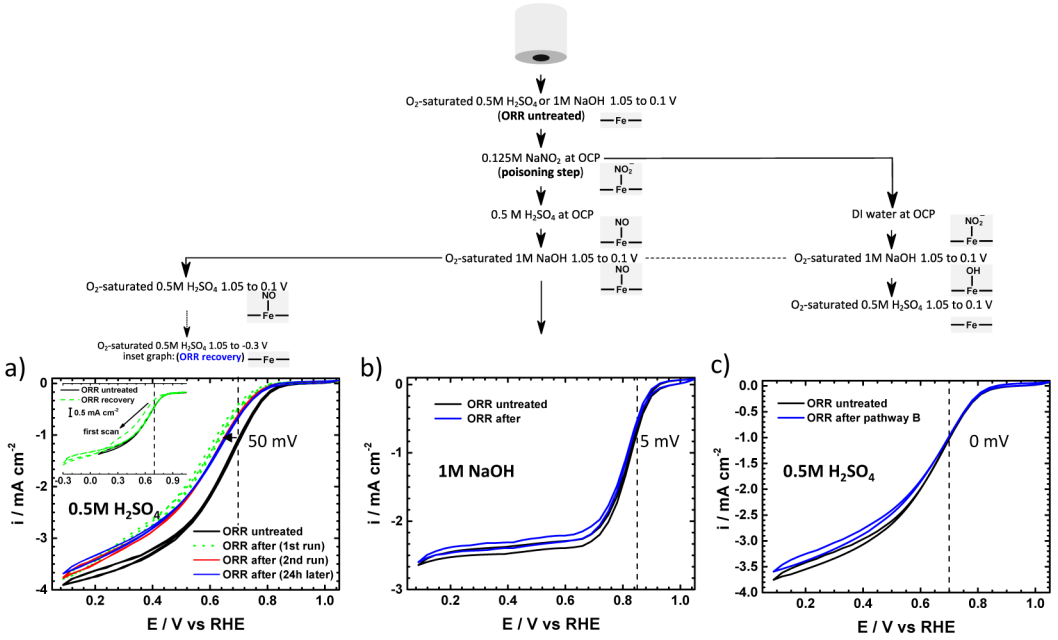

Figure 2. Rotating disk electrode (RDE) measurements in O_2-saturated 0.5 M H_2SO_4 of the ORR activity of a Fe−N/C catalyst before (untreated) and after poisoning by a 0.125 M $NaNO_3$ solution at pH 7. (a) Performance toward the ORR after acid wash following nitrite treatment and then cycling in 1 M alkaline solution before returning to acid solution to perform the ORR. Inset: Effect of shifting cathodic end point to −0.3 V. (b) Performance toward the ORR after DI water wash following the poisoning protocol and then cycling in 1 M alkaline solution before returning to acid solution to perform the ORR. (c) Performance to the ORR after DI water wash following nitrite treatment and then cycling in 1 M alkaline solution before returning to acid solution to perform the ORR. Conditions include RDE at 1600 rpm, catalyst loading at 270 μg cm^{-2}, and scan rate at 5 mV/s. "Pathway" refers to the pathways in Scheme 2.

would have been visible in the microscopy images at this resolution.[2,57,58] The iron content in the catalysts was determined by total reflection X-ray fluorescence spectroscopy (TXRF) to be 1.5 wt % and 60 ppm for the Fe−N/C and the N/C catalyst, respectively (see Supporting Information section S2).

In order to gain further information on the chemical behavior of the active site, a set of experiments were performed with inspiration taken from metal macrocyclic complexes, which are known to interact with nitrite and nitric oxide. In order to understand the poisoning effect of these species on the active site, the Fe−N/C catalyst deposited onto a glassy carbon rotating disk electrode (RDE) disk was assessed for oxygen reduction reaction (ORR) activity in 0.5 M H_2SO_4 or in 1 M NaOH both before and after treatment with the poisons under neutral pH conditions, as illustrated in Figure 1. It can be seen that there is significant poisoning of the activity of the catalyst under acidic conditions, whereas under alkaline conditions the effect is almost unnoticeable. It is known that the ORR activity significantly improves when moving to alkaline conditions.[59,60] The fact that no significant poisoning is seen under alkaline conditions, after exposure of the catalyst to the same treatment regime as for the acidic activity, might indicate that the active sites present under alkaline and under acid are fundamentally different. If the alkaline active site is not active or has only a low activity in acid and we assume a site which promotes an inner sphere electron transfer, it would be desirable to find ways to prevent the formation of this alkaline active site and promote the formation of the site which is highly active in acid if the catalyst is to be used in a proton exchange membrane fuel cell (and vice versa if it is to be used in an alkaline fuel cell). The presence of low activity sites will occupy space on the catalyst surface which could otherwise be occupied by highly active sites, suggested in recent literature, via ex situ techniques, to be an atomic iron center.[17,18,20,21,26,61] This dilution of highly active sites would make it difficult to reach the required active site density with the necessary turnover frequency.[15,62] Using the present probe in combination with physical characterization methods might enable a differentiation of sites.

As one of the major possible uses for these catalysts is in PEFCs based on acidic membranes, and as the largest effect on the ORR on these catalysts is seen under acidic conditions, we will predominantly confine the rest of our experiments to consider the ORR in acid.

3.2. Interaction of the Fe−N/C Catalyst with Nitrite. In Figure 2, we consider the stability of the poisoning species formed after exposure to nitrite to (a) variations of pH, (b) potential cycling in the ORR region, and (c) extended periods at the OCV. Figure 2a shows that the poison forms when the electrode is immersed in the nitrite solution at pH 7 and then washed with an acid solution. Once the acid wash is performed, exposure of the electrode to alkaline solution (and even performing the ORR in alkaline solution) does not recover the activity; there is still a 50 mV loss in performance. This performance loss is also stable to extended cycling under ORR conditions (between 1.05 and 0.1 V vs RHE), and leaving the electrode in solution at its OCV for 24 h. Thus, the poisoning species, once formed, is quite stable. However, it can be removed by cycling the potential to −0.3 V at which potential the poisoning species is reductively desorbed and the ORR activity recovered (Figure 2a, inset). However, poisoning of the electrode has neglible impact on the ORR in alkaline, Figure 2b.

In contrast, if instead of washing the electrode in acid solution after exposure to nitrite, the electrode is washed with water and then exposed to alkaline solution, the ORR performance is immediately recovered on cycling in acid,

DOI: 10.1021/jacs.6b09622
J. Am. Chem. Soc. 2016, 138, 16056−16068

Figure 2c. This highlights the requirement for the adsorbed nitrite to be exposed to acid solution in order to form the stable adduct on the site active for the ORR in acid.

The responses in Figure 2a–c are rationalized in Scheme 2. After treatment of the catalyst with nitrite solution, water wash,

Scheme 2. Proposed Reaction Steps of the Fe–N/C Active Site after Treatment with a Nitrite Containing Solution and Subsequent Treatment under Different pH Conditions

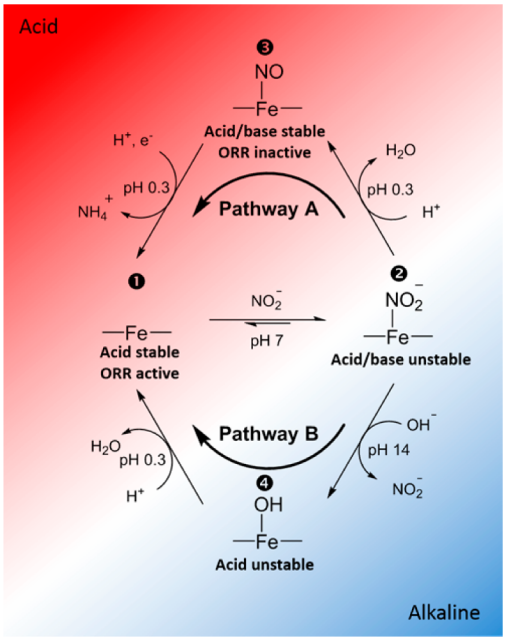

immersion of the nitrite complexed Fe–N/C catalyst **2** into an acidic solution (0.5 M H_2SO_4) forms poisoned species **3** (see results in Figure 2a). This species is stable in alkaline solution, as shown from the protocol used in Figure 2a in which the poisoned electrode is cycled in alkaline solution before returning to acid solution to perform the ORR results displayed. These steps seem to be associated with the decomposition of the nitrite ligand, which is only weakly bound, to form a nitrosyl complex **3**, which is bound with significantly more strength. The lower bond strength of a nitrite (~13–17 kJ mol^{-1})[63] compared to that of a nitrosyl ligand (~17–126 kJ mol^{-1})[64] is documented for iron heme based complexes and enzymes. Furthermore, for iron macrocyclic complexes, it has been shown that the nitrite ligand can be converted to nitrosyl upon reaction with protons and removal of water.[65] Only when the potential is sufficiently cathodic (Figure 2a, inset) is the nitrosyl complex reductively desorbed from the surface. Interestingly, once formed, poisoned complex **3** is also stable when extensively cycled in an oxygen-saturated alkaline solution (0.1 M NaOH) and then transferred back into the acid solution to perform the ORR reaction (see section S4 in SI).

In contrast, if complex **2** is immersed in alkaline solution after washing, the ORR activity in acid is immediately regenerated, Figure 2c. This confirms that, upon treatment with acid, a different species is formed. It also suggests that, due to the absence of free protons, the nitrite ligand was exchanged during the cycling in alkaline solution before a strong nitrosyl species is formed. As iron interacts strongly with hydroxide, as can be seen from the formation of stable hydroxides,[66] it would thus seem likely that hydroxo species **4** displaces the nitrite. Subsequent immersion in acid then regenerates the unpoisoned active site **1**. These experiments point toward an iron center as active site in acidic electrolyte. While the nitrite ligand is only weakly bound to the active site and can be replaced by the relatively strong hydroxo ligand, the nitrosyl ligand, which forms upon acid treatment, is significantly stronger and will not be replaced (Figure 2a,b and Figure S4). It also suggests that the iron center is not accessible as an active site in strongly alkaline solutions. This is supported by the fact that catalysts completely devoid of metal have been reported with high activities in alkaline electrolytes but not in acid.[67–69] It has to be pointed out that a "metal free" catalyst was weakly affected by nitrite (see Supporting Information section S5). This minor effect is likely due to the residual metal content which exists even in nominally "metal free" materials (see Supporting Information section S2). As the active site adduct **3** can be reductively destroyed, it allows us to use this technique to "count" the number of active metal centers. To our knowledge, this is the first account of the use of a probe with electrochemical recovery on this type of catalyst. The development of a stripping technique to exploit this behavior and count active sites is the subject of another paper.[60] As will be shown below, the product of the electrochemical reduction of the nitrosyl adduct is predominantly ammonia.

3.3. Interaction of the Fe–N/C Catalyst with Nitric Oxide. As has already been seen in Figure 1c,d, nitric oxide has a similar effect on the ORR performance as nitrite, barely affecting the performance in alkaline electrolyte, but having a significant effect in acid. Hence, in order to confirm whether a strongly bound nitrosyl compound is the poisoning species, the catalyst coated electrode was subjected to a saturated solution of nitric oxide in a pH 7 phosphate buffer for 5 min at a rotation of 300 rpm, Figure 3. As with the previous experiments, the stability of the adduct formed was studied as a function of (a) immersion in acid solution, (b) cycling in alkaline solution, and (c) cycling into a deeply reducing potential.

Again, two different pathways (post-poisoning), an acid one and an alkaline one, have been followed as shown in Figure 3 and interpreted in Scheme 3. In the acid pathway (Figure 3a), the catalyst was subjected to acid, before cycling in alkaline and then performing the ORR in acid again. After this treatment, the ORR activity did not recover. Interestingly the catalyst could be recovered in the same way as the nitrite treated adduct (Figure 2 a inset) by scanning to a lower potential and reductively stripping off the adduct. This suggests that the active site complex formed with nitrite in acid (**3**) and the stable intermediate formed with nitric oxide (**3′**, **3″**) are the same and supports the hypothesis of the formation of a nitrosyl complex upon acid treatment. If the nitrosyl complex indeed is present and is the stable species, it should form without acid treatment and survive the cycling in alkaline electrolyte. Therefore, the same experiments were performed in alkaline media, Figure 3b. In this experiment, after being subjected to nitric oxide in the pH 7 buffer and subsequent DI water wash, the catalyst was cycled in 1 M NaOH leading to **3‴**. It was found that, with nitric oxide, the stable complex **3‴** forms without acid treatment, as can be seen from the decreased ORR performance (Figure 3 b). Again, the performance can be recovered under low potential. This suggests that the same complex is formed upon nitric oxide treatment (**3′**, **3″**, **3‴**) and nitrite/acid treatment (**3**). The interaction of the catalyst with

DOI: 10.1021/jacs.6b09622
J. Am. Chem. Soc. 2016, 138, 16056–16068

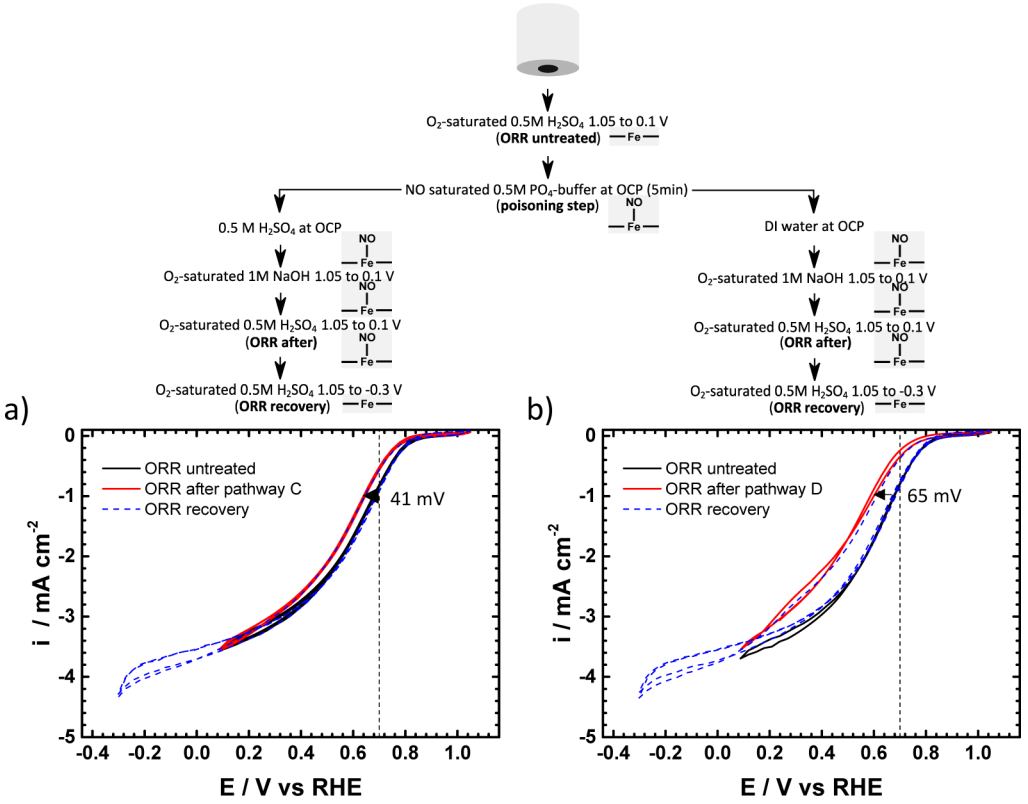

Figure 3. Rotating disk electrode (RDE) measurements in O_2-saturated 0.5 M H_2SO_4 of the ORR activity of a Fe−N/C catalyst before (untreated) and after poisoning in a saturated nitric oxide/0.5 M PO_4 buffer solution at pH 7. Performance toward the ORR after (a) acid washing and then cycling in 1 M alkaline solution before returning to acid solution to perform the ORR or (b) DI water washing and then cycling in 1 M alkaline solution before returning to acid solution to perform the ORR. In both cases the effect of extending the potential sweep to −0.3 V is also displayed. Conditions include 1600 rpm, loading 270 μg cm^{-2}, 5 mV/s, electrolyte 0.5 M H_2SO_4, O_2-saturated electrolyte. "Pathway" refers to the pathways in Scheme 3.

Scheme 3. Proposed Reaction Steps of the Fe−N/C Active Site after Treatment with Nitric Oxide at pH 7 and Subsequent Treatment under Different pH Conditions

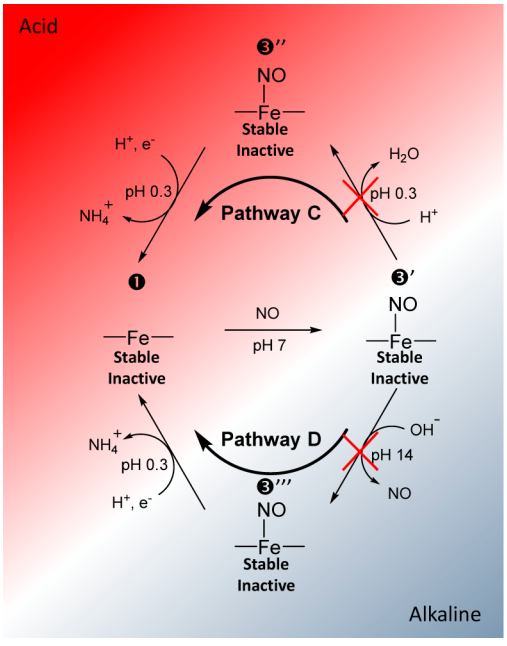

nitric oxide was then investigated in more depth in order to assess whether interpretable differences could be found.

In this case, the catalyst (deposited on a RDE) was poisoned by immersion in an acidified NO solution (instead of the pH 7 solution) described above), Figure 4. Two different cases were considered. In the first the electrode was poisoned by immersion at OCV, Figure 4a; in the second, it was poisoned by electrochemical cycling in the acidified NO solution, Figure 4b. When the electrode was poisoned at the open circuit potential at 300 rpm for 10 min and subsequently washed in DI water, there is a clear poisoning effect which is significantly stronger (~170 mV compared to ~41 to ~ 65 mV) than previously observed when the catalyst was subjected to nitric oxide at pH 7 for 5 min (Figure 3).

Possibly, this is due to the formation of other intermediates, **4** or **5** in Scheme 4, formed due to the change in open circuit potential caused by the pH shift (pH 7 compared to pH 0.3). Nevertheless, full recovery is still possible for these proposed poisoned species if the potential is reduced low enough to allow reductive stripping. However, the full recovery requires a change of electrolyte this time, which was not necessary before. It might be possible that a second set of active sites is poisoned during this protocol or the product that is stripped off at low potentials contaminates the electrolyte due to a higher concentration, which might not have been the case before (e.g., ammonium trapped at the sulfonate groups of the Nafion binder). However, when the electrode is cycled in acidified NO containing electrolyte between 1.05 and −0.3 V versus RHE (Figure 4b), no recovery was possible. Even extensive cycling to low potentials and the change of electrolyte could not recover

DOI: 10.1021/jacs.6b09622
J. Am. Chem. Soc. 2016, 138, 16056−16068

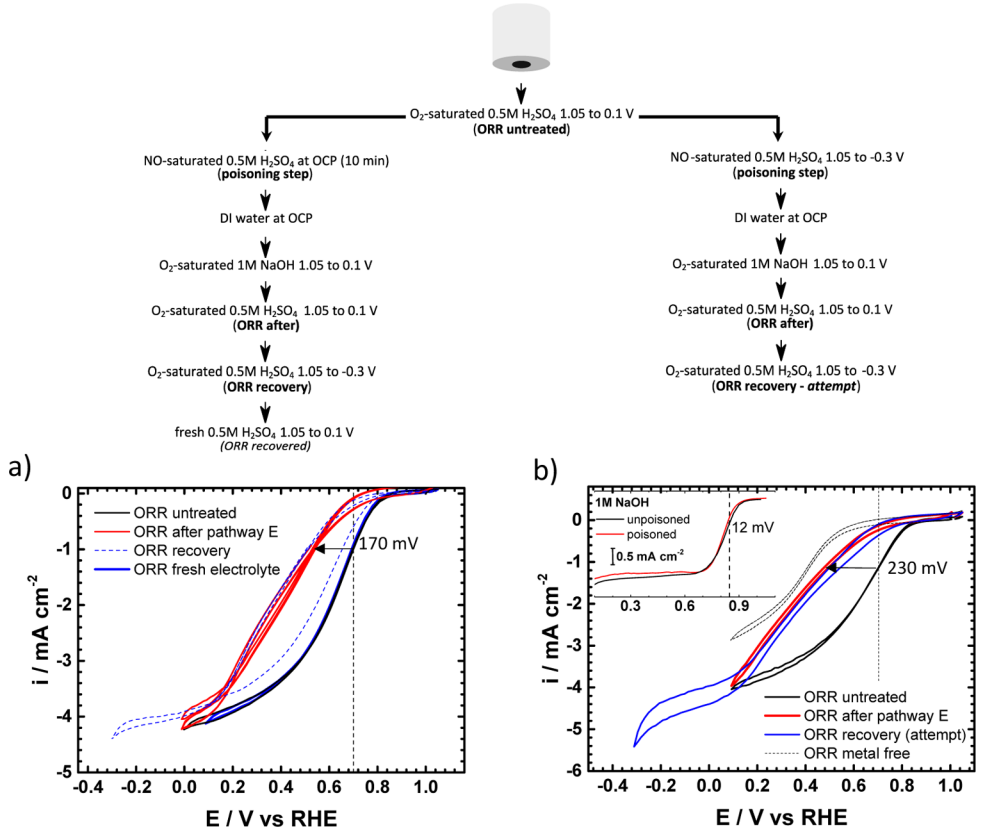

Figure 4. Rotating disk electrode (RDE) measurements in O_2-saturated 0.5 M H_2SO_4 of the ORR activity of a Fe−N/C catalyst before (untreated) and after poisoning in a saturated nitric oxide 0.5 M H_2SO_4 solution: (a) effect of poisoning the electrode at OCV; (b) effect of poisoning the electrode by performing cyclic voltammetry (1.05 V to −0.3 V) in the nitric oxide/0.5 M H_2SO_4 solution. Inset: ORR response of electrode in 1 M NaOH. In both cases the effect of extending the potential sweep to −0.3 V is also displayed. Conditions include the following: 1600 rpm, loading 270 μg cm^{-2}, 5 mV/s, electrolyte 0.5 M H_2SO_4, and O_2-saturated electrolyte. "Pathway" refers to the pathways in Scheme 4.

Scheme 4. Proposed Reaction Steps and Active Site Species Formed When Subjecting the Catalyst to an Acidic NO Solution, without Electrochemical Cycling (Pathway E) and with Electrochemical Cycling (Pathway F)

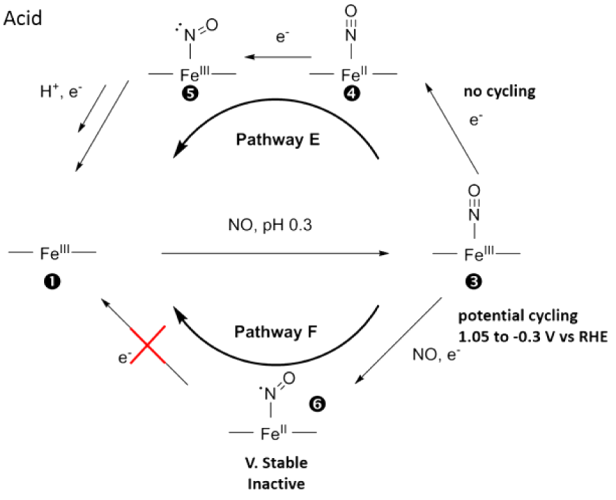

the electrode. Interestingly, the activity decrease is even larger as compared to that for the OCP case (Figure 4a) (~230 mV vs ~170 mV). Indeed, the poisoned catalyst approaches the activity of the nominally metal free N/C catalyst. This might indicate that almost all the metal induced active sites are poisoned (e.g., formation of **6**) or leached out. Interestingly, the alkaline activity of the strongly poisoned compared to the unpoisoned Fe−N/C catalyst is not significantly different (only a 12 mV shift in half-wave potential) as can be seen in the inset in Figure 4b. This again supports the hypothesis of a non-metal-centered active site in alkaline electrolyte, even if metal sites are present in the material. Ramaswamy et al. suggested an outer sphere electron transfer mechanism on this type of catalyst in alkaline electrolyte.[19] This means that even if the metal is covered by hydroxyl or nitrosyl, it still might be able to contribute to the activity. The irreversible poison effect observed in Figure 4b could be interpreted as the formation of an even more stable nitrosyl species (**6**) which acts as a kinetic dead end.[17,70,71] For iron complexes, two different conformations of nitrosyl ligation are possible: the linear form (**4**) and the bent form (**6**).[70,72] However, further experiments would be necessary to confirm this hypothesis. Severe degradation of the active site might also be considered. The use of nitrite and nitrosyl in combination with ex situ characterization methods such as X-ray absorption spectroscopy, Mössbauer spectroscopy, and electron spin resonance might enable insight into the underlying phenomena and differentiation among metal centered active sites.

3.4. Interaction of the Fe−N/C Catalyst with Hydroxylamine. As can be seen in Scheme 1, hydroxylamine (as NH_3OH^+ in the acidic electrolyte) is an intermediate in the nitrite/nitric oxide reduction pathway to ammonia,[38] analogous to peroxide being a potential intermediate for the ORR to water. It is known that hydroxylamine interacts with iron

DOI: 10.1021/jacs.6b09622
J. Am. Chem. Soc. 2016, 138, 16056−16068

macrocyclic complexes and also that it decomposes upon contact with transition metal ions.[73] This behavior is similar to that of hydrogen peroxide.[74] We probed the effect of hydroxylamine treatment on the catalyst to gain further information, Figure 5.

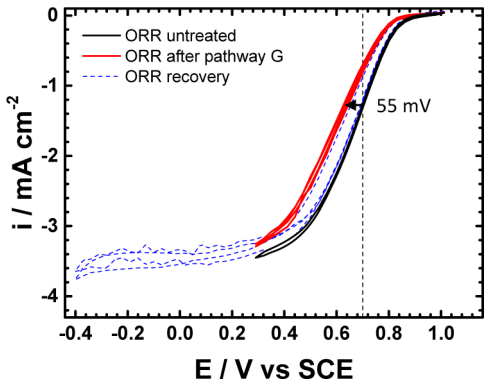

Figure 5. ORR performance before and after treatment in a 125 mM hydroxylamine solution at pH 7. A clear poisoning effect is present, which can be recovered by reductive cycling. Conditions include the following: 1600 rpm, loading 270 μg cm^{-2}, 5 mV/s, electrolyte 0.5 M pH 7 phosphate buffer, and O_2-saturated electrolyte. "Pathway" refers to the pathways in Scheme 5.

After determination of the original activity in a pH 7 phosphate buffer, the electrode was subjected to a neutral solution of hydroxylamine and then washed in DI water. In order to avoid the acidic decomposition, the ORR was then carried out at pH 7 in a phosphate buffer, so the electrode was never in contact with an acidic solution. Figure 5 shows that the same behavior of poisoning and recovery is observed as for NO treatment in alkaline and acid (in the absence of potential cycling).

This same poisoning effect as seen for nitrite suggests the formation of the same nitrosyl complex (**3**, in Scheme 5). This

Scheme 5. Proposed Reaction Steps of the Active Site upon Contact with Hydroxylamine and Subsequent Electrochemical Recovery

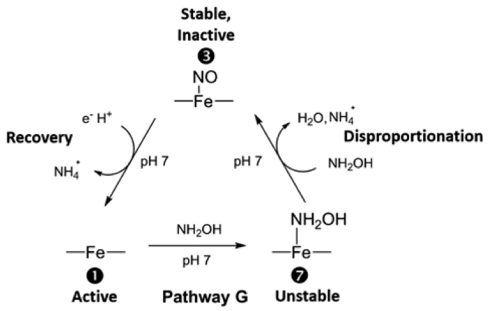

can be explained by a spontaneous disproportionation of hydroxylamine to form NO and water which is reported for the contact of hydroxylamine with transitions metals or heme complexes.[73,75] It further supports the similarity of the active site to iron macrocyclic complexes or at least metallic centers.

3.5. Effect of the Poison on the Cyclic Voltammetry of the Fe−N/C Catalyst. When cyclic voltammetry is performed on this type of catalyst in the absence of oxygen, many iron containing catalysts exhibit a reversible redox peak at around 0.6−0.8 V versus RHE.[19,76] As many metal free catalysts do not exhibit this peak, some publications associate the peak with the metal centered Fe^{2+}/Fe^{3+} redox peak of the active site.[19,76] It has to be pointed out that this peak can also be associated with a quinone/hydroquinone couple on the carbon surface.[77] Nevertheless, it is peculiar that a catalyst devoid of metal and prepared in the same way does not exhibit this peak. Ramaswamy et al. reported a relationship with the position of the redox peak and the activity of the catalyst.[19] The charge associated with this peak was used to determine the number of active sites and hence the site density. In a comparison of our Fe−N/C catalyst with the metal free catalyst N/C (Figure 6 a), it becomes apparent that the metal free catalyst does not exhibit this reversible redox peak, while the metal containing catalyst does. Therefore, the effect of the poison on this peak was investigated. De Groot et al. investigated iron heme compounds and iron containing enzymes, which were immobilized on electrodes, for their interaction with nitric oxide and its catalytic activity toward NO reduction.[44,45] They also investigated the redox behavior and the effect of the formation of a nitrosyl complex on the Fe^{2+}/Fe^{3+} redox peak and found that this peak is suppressed upon exposure to nitric oxide. If the redox peak was associated with the iron center which serves as an active site, we might expect some effect on the position or magnitude of the peak. However, it can be seen in Figure 6a that the Fe−N/C catalyst cycled in a 3 mM nitrite containing solution, which significantly affects the catalytic activity (210 mV potential shift, see Supporting Information section S10), shows no significant effect on the alleged Fe^{2+}/Fe^{3+} peak. Furthermore, an irreversibly poisoned Fe−N/C catalyst, which almost completely loses its metal centered activity (230 mV potential shift see Figure 4b), also shows no significant change in this peak (Figure 6b). The slight change in capacitance of the catalyst after pathway F (Figure 6b) is likely due to oxidation of the carbon surface by nitric oxide. However, the redox peak is unaffected. There are different possibilities as to this behavior: (i) The peak is not associated with the metal redox peak and/or the catalytic activity whatsoever. It might arise due to the quinone/hydroquinone couple. The addition of metal merely increases the concentration of this species. (ii) The peak is associated with metallic active sites that are significantly less active toward the ORR and do not interact with the poison. Other sites, which do interact with oxygen, also interact with nitrite and nitric oxide, but they are significantly in the minority and hence not seen in these experiments. (iii) The species associated with the peak is buried within the material and has no access to the surface and hence the poison. It might or might not influence the activity indirectly via long-range effects. A better understanding of this phenomenon might lead to better catalysts and should be investigated further.

3.6. Nitrite Electroreduction to Ammonia. As the Fe−N/C catalyst interacts strongly with nitrite, it is worthwhile considering whether it would be active toward the electroreduction of that compound. This could on one hand provide more information on the active site and on the other hand be useful in itself, as nitrite is an environmental pollutant and important biological messenger molecule.[38,39]

Figure 7a−c compares the catalytic activity of the Fe−N/C and the N/C catalysts at different pH values toward nitrite reduction. Figure 7a−c shows rotating disk electrode measurements of the catalysts in 3 mM $NaNO_2$ containing buffer solutions at pH 5.2, 7, and 9, respectively. It can be clearly seen that the Fe−N/C catalyst is active toward the reduction of

DOI: 10.1021/jacs.6b09622
J. Am. Chem. Soc. 2016, 138, 16056−16068

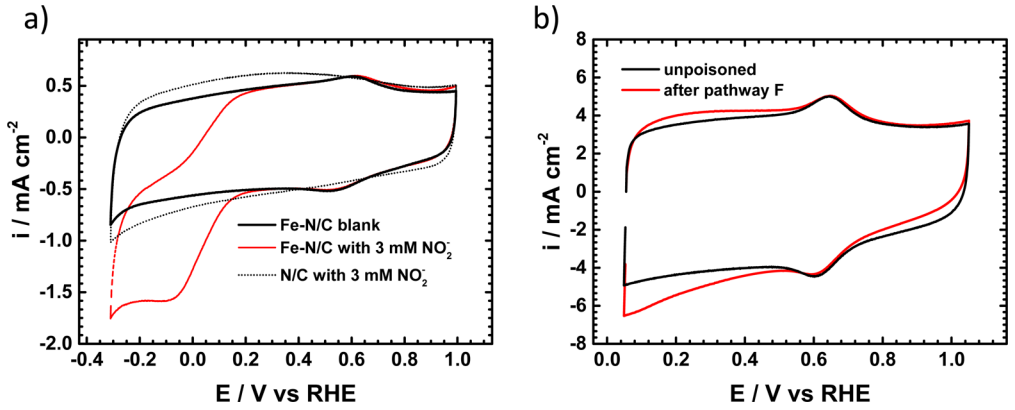

Figure 6. Cyclic voltammetry of the Fe−N/C and N/C catalysts in nitrogen-saturated electrolyte, comparing the voltammetry in the presence and absence of free nitrite and with strongly adsorbed intermediates. (a) Voltammetry of free nitrite in the electrolyte (3 mM $NaNO_2$ in pH 5.2 acetate buffer, 10 mV/s) and (b) voltammetry of Fe−N/C catalyst in NO-free solution (0.5 M H_2SO_4, 100 mV/s) before and after poisoning the surface (see pathway F in Scheme 4). Conditions include 1600 rpm, loading 270 μg cm^{-2}, and N_2-saturated electrolyte.

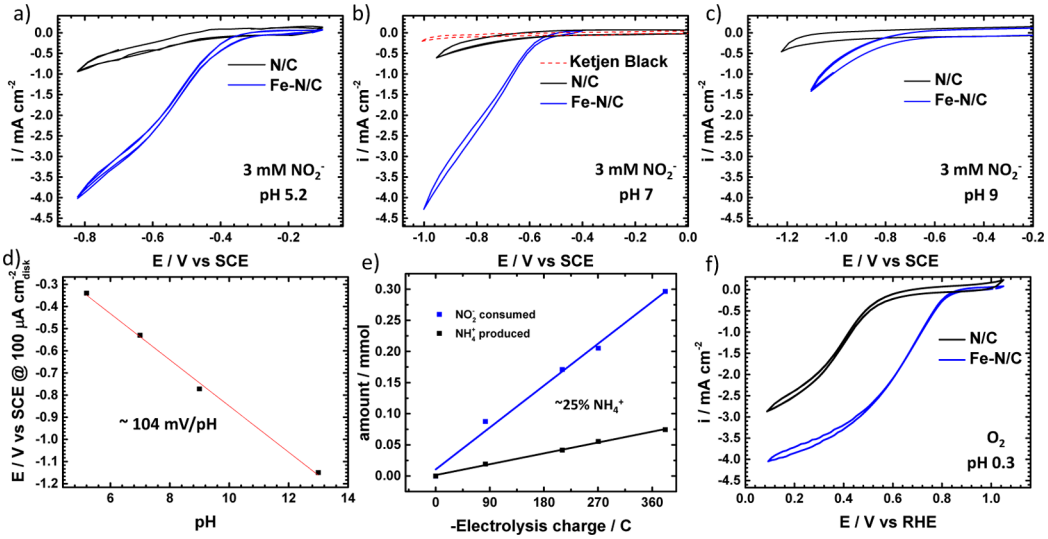

Figure 7. Rotating disk electrode measurements of a metal free catalyst N/C and an iron containing catalyst Fe−N/C toward nitrite reduction as a function of pH. (a−c) 3 mM $NaNO_2$ containing N_2-saturated electrolyte: (a) pH 5.2 acetate buffer, (b) pH 7 phosphate buffer, and (c) pH 9 borate buffer. (d) pH dependence of the corrected potential at 0.1 mA cm^{-2} toward nitrite reduction on the Fe−N/C catalyst. (e) Ion chromatographic ammonia yield and nitrite consumed versus charge for electrolysis of 10 mM potassium nitrite in 50 mM potassium acetate buffer at pH 5.2 at a potential of −0.55 V (SCE). (f) Measurement in O_2-saturated 0.5 M H_2SO_4. Conditions include the following: 1600 rpm, loading 270 μg cm^{-2}, and 5 mV/s.

nitrite. The onset potentials are approximately −0.3 V versus SCE (~0.2 V vs RHE), −0.5 V versus SCE (0.1 V vs RHE), and −0.8 V versus SCE (−0.08 V vs RHE), respectively.

Interestingly, these overpotentials are significantly lower than the ones reported by Duca et al. for hemin adsorbed on pyrolytic graphite.[78] Therefore, the pyrolyzed catalyst is significantly more active than unpyrolyzed iron heme centers. Strikingly, this is analogous to the effect of heat treatment of heme based systems on the activity toward the oxygen reduction reaction.[11,12] It can also be seen that the N/C catalyst, while still showing some activity, requires an extra overpotential over the Fe−N/C catalyst of −230, −295, and −355 mV, respectively. This is interesting, as this shift in overpotential is similar to the difference in the oxygen reduction reaction in acid electrolyte on these catalysts (about 265 mV, Figure 7f). This will enable further investigations into the nature of the active site while utilizing nitrite in combination with ex situ physical characterization methods, as mentioned above. It is also evident that the nitrite reduction becomes more sluggish at higher pH values. It shows a slope of ~104 mV/pH (Figure 7d), somewhat different from the 59 mV/pH unit expected for a simple proton coupled electron transfer. This indicates that a complicated multi-electron and multiproton reduction is expected for this process. Duca et al. showed that, for hemin adsorbed on pyrolytic graphite, the reduction of nitrite must occur via the decomposition of HNO_2 prior to electroreduction.[78] However, for the Fe−N/C catalyst shown here, this is not the case, as the concentration of HNO_2 is too low to be able to obtain the observed currents (see Supporting Information section S11). This is even more obvious at pH 7 and higher, where the observed currents are orders of magnitude higher than would be possible with the concentration of HNO_2 in solution (see Supporting Information section S11). We therefore infer that the catalyst is capable of activating the unprotonated nitrite molecule. Even at pH 14, the catalyst still exhibits significant

DOI: 10.1021/jacs.6b09622
J. Am. Chem. Soc. 2016, 138, 16056−16068

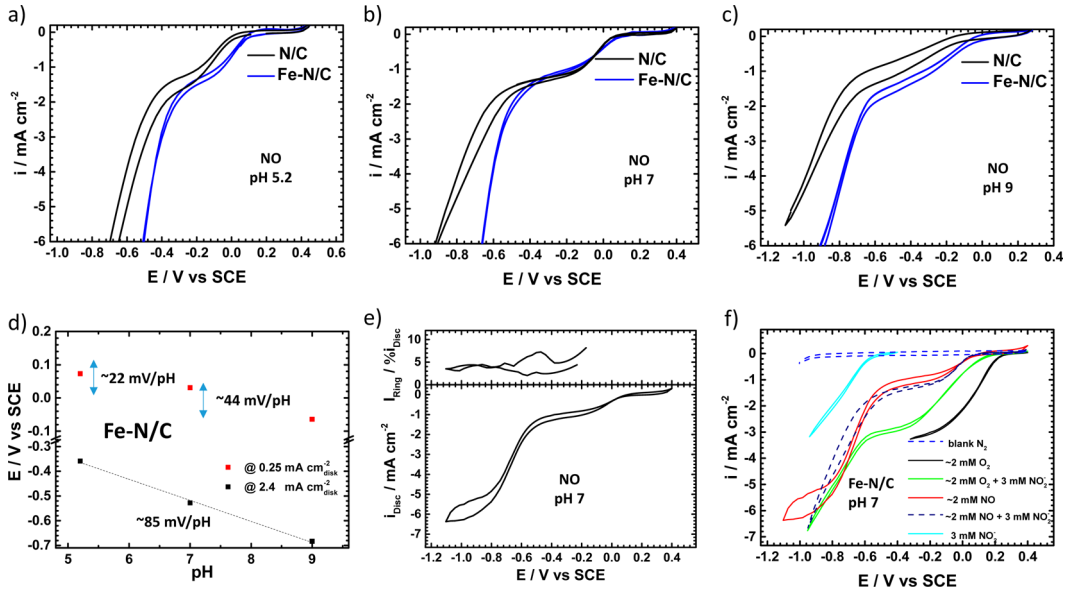

Figure 8. Rotating disk electrode (RDE) measurements of a metal free catalyst N/C and an iron containing catalyst Fe–N/C toward NO electroreduction as a function of pH. (a–c) NO-saturated electrolyte: (a) pH 5.2 acetate buffer, (b) pH 7 phosphate buffer, and (c) pH 9 borate buffer. (d) pH dependence of the potentials at 0.25 and 2.4 mA cm^{-2} toward NO reduction. (e) Rotating ring disk electrode measurement (RRDE) of a NO-saturated solution in pH 7 0.5 M phosphate buffer. (f) Rotating disk electrode measurement of the Fe–N/C catalyst with different substrates O_2, NO, and NO_2^-. Conditions include 1600 rpm, loading 270 μg cm^{-2}, and 5 mV/s.

activity toward nitrite reduction (see Supporting Information section S11), further supporting the ability of the catalyst to activate nitrite.

A Koutecky–Levich analysis (see Supporting Information section S12) at pH 5.2 and 7 indicates a high electron transfer number of 5.2 and 4.8, respectively. In order to achieve a better idea of the product distribution of this complex reaction, the hydroxylamine content was monitored via the rotating ring disk electrode (RRDE) with a Pt ring (see Supporting Information section S14). It was found to be below 5% at pH 5.2 and slightly higher at pH 7. The high electron transfer number and the low hydroxylamine content suggest the production of ammonia. Therefore, a long-term electrolysis experiment at an applied potential of −0.55 V (vs SCE) of 10 mM potassium nitrite in 50 mM potassium acetate buffer at pH 5.2 was performed, and the ammonia and nitrite content was followed over time with ion chromatography. Figure 7e shows the amount of ammonia produced and nitrite consumed versus the respective amount of charge passed (see Supporting Information section S15 for more details). It can be seen that the concentration of ammonia increases at about 1/4 the rate of nitrite decrease. The other 3/4 of the nitrite removal might be associated with the production of nitrogen (see Supporting Information). With the assumption of a 25:75% split between NH_4^+ and N_2, and eqs 1 and 2,

$$NO_2^- + 7H^+ + 6e^- \leftrightarrows NH_3 + 2\,H_2O \quad (1)$$

$$NO_2^- + 4H^+ + 3e^- \leftrightarrows N_2 + 2\,H_2O \quad (2)$$

the average charge consumed per molecule of nitrite converted would be n = 3.75, which is slightly lower than the average n value found in the RDE results above. This indicates that this complex reaction proceeds via different pathways (see Scheme 1). The low production of hydroxylamine and the high detected amount of ammonia is striking, as it would require that both N–O bonds are broken. This is not typical for simple iron-heme based catalysts, as they have been reported to produce close to 100% hydroxylamine and are not able to break the second N–O bond.[45] Either complex enzymes or precious metal based catalysts have been reported to produce ammonia depending on the conditions.[38]

3.7. Nitric Oxide Electroreduction and Possible Sensing Applications. The nitric oxide reduction reaction was examined at pH values of 5.2, 7, and 9 in order to gain further information, Figure 8a–c. It can be seen that the onset potential for NO reduction is shifted upward for both the Fe–N/C and N/C catalysts as compared to the nitrite reduction. Also striking is that the difference in overpotential between the two catalysts is significantly smaller than that for nitrite reduction (~83, ~5, and ~120 mV for pH 5.2, 7, and 9, respectively). This indicates that the nitric oxide molecule is activated differently as compared to the nitrite molecule, presumably on the metal containing active site as well as on another metal free site or on the doped carbon surface via an outer sphere mechanism. It is also apparent that the reductive wave shows a plateau for both the Fe–N/C and the N/C catalysts. This behavior was observed for NO reduction on precious metal catalysts but not for iron heme based systems, as they only showed a single reduction wave at significantly lower potentials (higher overpotentials).[45] In the case of the Fe–N/C catalyst, a plateau with a current of ~1.5 mA cm^{-2} is visible (Figure 8a–c) suggesting a one electron transfer, which would have a theoretical limiting current of 2.3 mA cm^{-2} (see Supporting Information section S16), and suggesting the reduction of NO to N_2O (see Scheme 1 and Supporting Information). Interestingly, De Groot et al. observe a similar shape with a reductive prewave at a current of 1.63 mA cm^{-2} and at similar potentials, but on a Pt disk, and argued that this would correspond to a one electron reduction.[45] This puzzling result could have interesting implications on the different modes of activation toward small molecules in this type of material. The carbon catalyst might exhibit an electrocatalytically active surface that might be modified by different dopants in addition to distinct active sites. It is also striking that the N/

DOI: 10.1021/jacs.6b09622
J. Am. Chem. Soc. 2016, 138, 16056–16068

C catalyst performs not significantly worse than the Fe−N/C catalyst. Moreover, it shows a similar shape of a reductive prewave. This suggests indeed a different activation of NO as compared to nitrite. Investigating the effect of pH on the two reductive waves shows that the first wave exhibits a very low pH dependence (∼20−40 mV/pH) of the potential at which a kinetic current of 0.25 mA cm^{-2} is achieved (Figure 8 d). Such low values are significantly smaller than the expected 59 mV/pH when a proton is involved in the rate-determining step. This indicates a proton independent slow step. In contrast, the second wave shows a much larger pH dependence of ∼85 mV/pH. The values for the N/C catalyst are ∼18 and ∼100 mV/pH, respectively (see Supporting Information section S16). For the N/C catalyst the second wave however shows a slope of ∼100 mV/pH, which again suggests a strong pH dependence, similar to the nitrite reduction. It can also be seen that the difference in overpotential between Fe−N/C and N/C of the second wave is smaller when compared to nitrite reduction. This also suggests that the second wave for the nitric oxide reduction has a contribution from the metal free activity and the metal containing site. This makes NO in combination with nitrite and ex situ characterization methods a powerful approach to probe the different active sites. Further insight might be gained by investigating the product distribution in more detail, with studies such as differential electrochemical mass spectrometry (DEMS), as has been done for other catalysts.[48]

Sensors which can simultaneously determine nitric oxide, nitrite, and oxygen would be desirable for biological systems, due to the importance of these molecules in regulating metabolic functions.[39,51−53,64,79] The voltammetric response of the Fe−N/C catalyst to different combinations of substrates in the electrolyte is shown in Figure 8 f. The response of the catalyst toward the different substrates has been probed with the rotating disk electrode at 1600 rpm under physiological conditions in a pH 7 phosphate buffer. It can be clearly seen that there are significant differences. In the absence of any reactive substrate, under nitrogen, the catalyst does not show any current in a wide potential window. When the electrolyte is saturated with pure oxygen, it exhibits a clear wave with an onset potential of ∼0.24 V versus SCE. A solution of 3 mM nitrite in the absence of oxygen (nitrogen saturation) shows a reductive wave with an onset potential of −0.56 V versus SCE. Importantly, the reductive wave is significantly different from the response for pure nitric oxide, which shows a prewave at higher potential (0.08 V vs SCE onset potential) and a limiting current at lower potential (approximately −1.0 V vs SCE). The combination of nitrite and nitric oxide shows a similar response to pure nitric oxide but without a limiting current. This makes it possible to differentiate between nitrite and nitric oxide and even distinguish between pure nitric oxide and the combination of both. Finally, the combination of nitrite and oxygen shows again a different response with a first wave associated with oxygen reduction, an onset potential of ∼0.16 V versus SCE, and a second wave associated with nitrite reduction starting at approximately −0.53 V versus SCE. This specific behavior could be exploited for sensors in biological systems.

4. CONCLUSIONS

Here, we demonstrated that a heat treated Fe−N/C catalyst interacts strongly with nitrite, nitric oxide, and hydroxylamine. The catalyst was exposed to different treatments after the poisoning step allowing formation of either a weakly bound nitrite complex or a significantly stronger nitrosyl complex with, presumably, an iron centered active site. These species are stable toward electrochemical cycling and time, but can be recovered (i.e., removal of adsorbate) if cycled to low potentials. With nitric oxide, there is the possibility to form a species which cannot be removed by electrochemical treatment. This behavior is an indication for a set of active sites with similar behavior to iron heme. Utilizing these probes, a more in-depth analysis is now possible. The Fe−N/C catalyst is highly active toward reduction of nitrite, showing a large difference compared to the activity the metal free N/C catalyst. This difference in activity mirrors their oxygen reduction reaction performance. In contrast to iron heme complexes, which predominantly form hydroxylamine during nitrite reduction, i.e., not breaking the second N−O bond, the Fe−N/C catalyst forms ammonia as a significant byproduct and hence appears to be able to break both N−O bonds. While iron heme complexes cannot activate unprotonated nitrite, the Fe−N/C catalyst does catalyze the reduction even at high pH values. This behavior is similar to complex enzymes or precious metal surfaces. The nitric oxide reduction shows a different behavior with two reductive waves similar to precious metal surfaces. This study offers insight into the chemical behavior of the active site and a new probe for further investigation through ex situ methods. This might facilitate the identification of key features of highly active sites and the improvement of this type of catalyst. The significant difference in the response toward nitrite, nitric oxide, and oxygen might inspire the development of new sensors for biochemical and environmental applications.

■ ASSOCIATED CONTENT

Supporting Information

The Supporting Information is available free of charge on the ACS Publications website at DOI: 10.1021/jacs.6b09622.

Additional characterization details, experimental details, and analyses (PDF)

■ AUTHOR INFORMATION

Corresponding Author

*anthony@imperial.ac.uk

ORCID

Anthony Kucernak: 0000-0002-5790-9683

Thiago Lopes: 0000-0002-1049-4679

Notes

The authors declare no competing financial interest.

The data used in the production of the figures in this paper are available for download at: DOI: 10.5281/zenodo.167960.

■ ACKNOWLEDGMENTS

The authors would like to thank the U.K. Engineering and Physical Sciences research council under Project EP/J016454/1 for financial assistance. T.L. would also like to thank the Sao Paulo Research Foundation under project 2016/07848-3 for T.L.'s fellowship and Projects 2014/50279-4 and 2014/09087-4 for financial assistance. The authors gratefully acknowledge helpful advice and discussions with Dr. Matthew Markiewicz.

■ REFERENCES

(1) Debe, M. K. *Nature* **2012**, *486*, 43.

(2) Wu, G.; More, K. L.; Johnston, C. M.; Zelenay, P. *Science* **2011**, *332*, 443.

DOI: 10.1021/jacs.6b09622
J. Am. Chem. Soc. 2016, 138, 16056−16068

(3) Jaouen, F.; Proietti, E.; Lefèvre, M.; Chenitz, R.; Dodelet, J.-P.; Wu, G.; Chung, H. T.; Johnston, C. M.; Zelenay, P. *Energy Environ. Sci.* **2011**, *4*, 114.
(4) Proietti, E.; Jaouen, F.; Lefèvre, M.; Larouche, N.; Tian, J.; Herranz, J.; Dodelet, J.-P. *Nat. Commun.* **2011**, *2*, 416.
(5) Lefèvre, M.; Proietti, E.; Jaouen, F.; Dodelet, J.-P. *Science* **2009**, *324*, 71.
(6) Shui, J.; Chen, C.; Grabstanowicz, L.; Zhao, D.; Liu, D.-J. *Proc. Natl. Acad. Sci. U. S. A.* **2015**, *112*, 10629.
(7) Jasinski, R. *Nature* **1964**, *201*, 1212.
(8) Jasinski, R. *J. Electrochem. Soc.* **1965**, *112*, 526.
(9) Jahnke, D. H.; Schönborn, D. M.; Zimmermann, D. G. In *Physical and Chemical Applications of Dyestuffs*; Schäfer, F. P., Gerischer, H., Willig, F., Meier, H., Jahnke, H., Schönborn, M., Zimmermann, G., Eds.; Springer: Berlin, 1976; p 133.
(10) van Veen, J. a. R.; Colijn, H. A. *Berichte der Bunsengesellschaft für physikalische Chemie* **1981**, *85*, 700.
(11) van Veen, J. A. r.; van Baar, J. F.; Kroese, C. J.; Coolegem, J. G. F.; De Wit, N.; Colijn, H. A. *Berichte der Bunsengesellschaft für physikalische Chemie* **1981**, *85*, 693.
(12) Yeager, E. *Electrochim. Acta* **1984**, *29*, 1527.
(13) Bagotzky, V. S.; Tarasevich, M. R.; Radyushkina, K. A.; Levina, O. A.; Andrusyova, S. I. *J. Power Sources* **1978**, *2*, 233.
(14) Shao, M.; Chang, Q.; Dodelet, J.-P.; Chenitz, R. *Chem. Rev.* **2016**, *116*, 3594.
(15) Gasteiger, H. A.; Kocha, S. S.; Sompalli, B.; Wagner, F. T. *Appl. Catal., B* **2005**, *56*, 9.
(16) Jaouen, F.; Herranz, J.; Lefèvre, M.; Dodelet, J.-P.; Kramm, U. I.; Herrmann, I.; Bogdanoff, P.; Maruyama, J.; Nagaoka, T.; Garsuch, A.; Dahn, J. R.; Olson, T.; Pylypenko, S.; Atanassov, P.; Ustinov, E. A. *ACS Appl. Mater. Interfaces* **2009**, *1*, 1623.
(17) Herranz, J.; Jaouen, F.; Lefèvre, M.; Kramm, U. I.; Proietti, E.; Dodelet, J.-P.; Bogdanoff, P.; Fiechter, S.; Abs-Wurmbach, I.; Bertrand, P.; Arruda, T. M.; Mukerjee, S. *J. Phys. Chem. C* **2011**, *115*, 16087.
(18) Kramm, U. I.; Herranz, J.; Larouche, N.; Arruda, T. M.; Lefèvre, M.; Jaouen, F.; Bogdanoff, P.; Fiechter, S.; Abs-Wurmbach, I.; Mukerjee, S.; Dodelet, J.-P. *Phys. Chem. Chem. Phys.* **2012**, *14*, 11673.
(19) Ramaswamy, N.; Tylus, U.; Jia, Q.; Mukerjee, S. *J. Am. Chem. Soc.* **2013**, *135*, 15443.
(20) Kramm, U. I.; Lefèvre, M.; Larouche, N.; Schmeisser, D.; Dodelet, J.-P. *J. Am. Chem. Soc.* **2014**, *136*, 978.
(21) Sahraie, N. R.; Kramm, U. I.; Steinberg, J.; Zhang, Y.; Thomas, A.; Reier, T.; Paraknowitsch, J.-P.; Strasser, P. *Nat. Commun.* **2015**, *6*, 8618.
(22) Tylus, U.; Jia, Q.; Strickland, K.; Ramaswamy, N.; Serov, A.; Atanassov, P.; Mukerjee, S. *J. Phys. Chem. C* **2014**, *118*, 8999.
(23) Kramm, U. I.; Herrmann-Geppert, I.; Behrends, J.; Lips, K.; Fiechter, S.; Bogdanoff, P. *J. Am. Chem. Soc.* **2016**, *138*, 635.
(24) Cooper, C. E.; Brown, G. C. *J. Bioenerg. Biomembr.* **2008**, *40*, 533.
(25) Strickland, K.; Miner, E.; Jia, Q.; Tylus, U.; Ramaswamy, N.; Liang, W.; Sougrati, M.-T.; Jaouen, F.; Mukerjee, S. *Nat. Commun.* **2015**, *6*, 7343.
(26) Ferrandon, M.; Kropf, A. J.; Myers, D. J.; Artyushkova, K.; Kramm, U.; Bogdanoff, P.; Wu, G.; Johnston, C. M.; Zelenay, P. *J. Phys. Chem. C* **2012**, *116*, 16001.
(27) Gupta, S.; Fierro, C.; Yeager, E. *J. Electroanal. Chem. Interfacial Electrochem.* **1991**, *306*, 239.
(28) Thorum, M. S.; Hankett, J. M.; Gewirth, A. A. *J. Phys. Chem. Lett.* **2011**, *2*, 295.
(29) Oberst, J. L.; Thorum, M. S.; Gewirth, A. A. *J. Phys. Chem. C* **2012**, *116*, 25257.
(30) Singh, D.; Mamtani, K.; Bruening, C. R.; Miller, J. T.; Ozkan, U. S. *ACS Catal.* **2014**, *4*, 3454.
(31) Wiesener, K. *Electrochim. Acta* **1986**, *31*, 1073.
(32) Ozaki, J.-i.; Anahara, T.; Kimura, N.; Oya, A. *Carbon* **2006**, *44*, 3358.
(33) Birry, L.; Zagal, J. H.; Dodelet, J.-P. *Electrochem. Commun.* **2010**, *12*, 628.
(34) Malko, D.; Lopes, T.; Symianakis, E.; Kucernak, A. R. *J. Mater. Chem. A* **2016**, *4*, 142.
(35) Wang, Q.; Zhou, Z.-Y.; Lai, Y.-J.; You, Y.; Liu, J.-G.; Wu, X.-L.; Terefe, E.; Chen, C.; Song, L.; Rauf, M.; Tian, N.; Sun, S.-G. *J. Am. Chem. Soc.* **2014**, *136*, 10882.
(36) Wayland, B. B.; Olson, L. W. *J. Chem. Soc., Chem. Commun.* **1973**, 897.
(37) Bard, A. J.; Parsons, R.; Jordan, J. *Standard Potentials in Aqueous Solution*; CRC Press, 1985.
(38) Rosca, V.; Duca, M.; de Groot, M. T.; Koper, M. T. M. *Chem. Rev.* **2009**, *109*, 2209.
(39) Pereira, C.; Ferreira, N. R.; Rocha, B. S.; Barbosa, R. M.; Laranjinha, J. *Redox Biol.* **2013**, *1*, 276.
(40) Silaghi-Dumitrescu, R.; Svistunenko, D. A.; Cioloboc, D.; Bischin, C.; Scurtu, F.; Cooper, C. E. *Nitric Oxide* **2014**, *42*, 32.
(41) Tsou, C.-C.; Yang, W.-L.; Liaw, W.-F. *J. Am. Chem. Soc.* **2013**, *135*, 18758.
(42) Silaghi-Dumitrescu, R. *Eur. J. Inorg. Chem.* **2003**, *2003*, 1048.
(43) Lundberg, J. O.; Weitzberg, E.; Gladwin, M. T. *Nat. Rev. Drug Discovery* **2008**, *7*, 156.
(44) de Groot, M. T.; Merkx, M.; Koper, M. T. M. *J. Am. Chem. Soc.* **2005**, *127*, 16224.
(45) de Groot, M. T.; Merkx, M.; Wonders, A. H.; Koper, M. T. M. *J. Am. Chem. Soc.* **2005**, *127*, 7579.
(46) Duca, M.; Figueiredo, M. C.; Climent, V.; Rodriguez, P.; Feliu, J. M.; Koper, M. T. M. *J. Am. Chem. Soc.* **2011**, *133*, 10928.
(47) Rosca, V.; Beltramo, G. L.; Koper, M. T. M. *Langmuir* **2005**, *21*, 1448.
(48) de Vooys, A. C. A.; Koper, M. T. M.; van Santen, R. A.; van Veen, J. A. R. *Electrochim. Acta* **2001**, *46*, 923.
(49) de Vooys, A. C. A.; Beltramo, G. L.; van Riet, B.; van Veen, J. A. R.; Koper, M. T. M. *Electrochim. Acta* **2004**, *49*, 1307.
(50) Koper, M. T. M.; van Santen, R. A. *J. Electroanal. Chem.* **1999**, *476*, 64.
(51) Zen, J. M.; Kumar, A. S.; Wang, H. F. *Analyst* **2000**, *125*, 2169.
(52) Boo, Y. C.; Mun, G. I.; Tressel, S. L.; Jo, H. *Methods Mol. Biol. (N. Y., NY, U. S.)* **2011**, *704*, 81.
(53) Hetrick, E. M.; Schoenfisch, M. H. *Annu. Rev. Anal. Chem.* **2009**, *2*, 409.
(54) Paulus, U. A.; Schmidt, T. J.; Gasteiger, H. A.; Behm, R. J. *J. Electroanal. Chem.* **2001**, *495*, 134.
(55) Schmidt, T. J.; Gasteiger, H. A.; Stäb, G. D.; Urban, P. M.; Kolb, D. M.; Behm, R. J. *J. Electrochem. Soc.* **1998**, *145*, 2354.
(56) Lewis, R. S.; Deen, W. M. *Chem. Res. Toxicol.* **1994**, *7*, 568.
(57) Wu, W.; Zhu, Z.; Liu, Z.; Xie, Y.; Zhang, J.; Hu, T. *Carbon* **2003**, *41*, 317.
(58) Deng, D.; Yu, L.; Chen, X.; Wang, G.; Jin, L.; Pan, X.; Deng, J.; Sun, G.; Bao, X. *Angew. Chem., Int. Ed.* **2013**, *52*, 371.
(59) Ramaswamy, N.; Mukerjee, S. *J. Phys. Chem. C* **2011**, *115*, 18015.
(60) Malko, D.; Kucernak, A.; Lopes, T. *Nat. Commun.* **2016**, *7*, 13285.
(61) Kramm, U. I.; Zana, A.; Vosch, T.; Fiechter, S.; Arenz, M.; Schmeißer, D. *J. Solid State Electrochem.* **2016**, *20*, 969.
(62) Lopes, T.; Kucernak, A.; Malko, D.; Ticianelli, E. A. *ChemElectroChem* **2016**, *3*, 1580.
(63) Fujii, H.; Yamaki, D.; Ogura, T.; Hada, M. *Chemical Science* **2016**, *7*, 2896.
(64) Hunt, A. P.; Lehnert, N. *Acc. Chem. Res.* **2015**, *48*, 2117.
(65) Einsle, O.; Messerschmidt, A.; Huber, R.; Kroneck, P. M. H.; Neese, F. *J. Am. Chem. Soc.* **2002**, *124*, 11737.
(66) Brookins, D. G. *Eh-pH Diagrams for Geochemistry*, softcover reprint of the original 1st (1988) ed.; Springer, 2011.
(67) Yang, Z.; Yao, Z.; Li, G.; Fang, G.; Nie, H.; Liu, Z.; Zhou, X.; Chen, X. a.; Huang, S. *ACS Nano* **2012**, *6*, 205.
(68) Zheng, Y.; Jiao, Y.; Chen, J.; Liu, J.; Liang, J.; Du, A.; Zhang, W.; Zhu, Z.; Smith, S. C.; Jaroniec, M.; Lu, G. Q. M.; Qiao, S. Z. *J. Am. Chem. Soc.* **2011**, *133*, 20116.

DOI: 10.1021/jacs.6b09622
J. Am. Chem. Soc. 2016, 138, 16056−16068

(69) Wang, S.; Zhang, L.; Xia, Z.; Roy, A.; Chang, D. W.; Baek, J.-B.; Dai, L. *Angew. Chem., Int. Ed.* **2012**, *51*, 4209.
(70) Blair, E.; Sulc, F.; Farmer, P. J. In *N4-Macrocyclic Metal Complexes*; Zagal, J. H., Bedioui, F., Dodelet, J.-P., Eds.; Springer: New York, 2006; p 149.
(71) Matsumura, H.; Hayashi, T.; Chakraborty, S.; Lu, Y.; Moënne-Loccoz, P. *J. Am. Chem. Soc.* **2014**, *136*, 2420.
(72) Zagal, J. H.; Bedioui, F.; Dodelet, J. P. *N4-Macrocyclic Metal Complexes*; Springer Science & Business Media, 2007.
(73) Bari, S. E.; Amorebieta, V. T.; Gutiérrez, M. M.; Olabe, J. A.; Doctorovich, F. *J. Inorg. Biochem.* **2010**, *104*, 30.
(74) Kim, S.-J.; Yoon, B.-H. *Journal of Korea Technical Association of The Pulp and Paper Industry* **2006**, *38*, 79.
(75) Pacheco, A. A.; McGarry, J.; Kostera, J.; Corona, A. *Methods Enzymol.* **2011**, *486*, 447.
(76) Chlistunoff, J. *J. Phys. Chem. C* **2011**, *115*, 6496.
(77) Kinoshita, K.; Bett, J. A. S. *Carbon* **1973**, *11*, 403.
(78) Duca, M.; Khamseh, S.; Lai, S. C. S.; Koper, M. T. M. *Langmuir* **2010**, *26*, 12418.
(79) Tsai, A.-L.; Berka, V.; Martin, E.; Olson, J. S. *Biochemistry* **2012**, *51*, 172.

DOI: 10.1021/jacs.6b09622
J. Am. Chem. Soc. 2016, 138, 16056−16068